

# Research Regimes and Design Optimization of JT-60SA Device towards ITER and DEMO

Y. Kamada<sup>1</sup>, P. Barabaschi<sup>2</sup>, S. Ishida<sup>3</sup>, S. Ide<sup>1</sup>, K. Lackner<sup>2</sup>, T. Fujita<sup>1</sup>, T. Bolzonella<sup>4</sup>,  
T. Suzuki<sup>1</sup>, G. Matsunaga<sup>1</sup>, M. Yoshida<sup>1</sup>, K. Shinohara<sup>1</sup>, H. Urano<sup>1</sup>, T. Nakano<sup>1</sup>,  
S. Sakurai<sup>1</sup>, H. Kawashima<sup>1</sup>, and the JT-60SA Team

<sup>1</sup> JT-60SA JA-Home Team, Japan Atomic Energy Agency, 801-1 Mukoyama, Naka, Ibaraki, Japan,

<sup>2</sup> JT-60SA EU-Home Team, Fusion for Energy, Boltzmannstr 2, Garching, 85748, Germany

<sup>3</sup> JT-60SA Project Team, 801-1 Mukoyama, Naka, Ibaraki, Japan,

<sup>4</sup> JT-60SA EU-Home Team, corso Stati Uniti 4, 35127 Padova, Italy

E-mail contact of main author: kamada.yutaka@jaea.go.jp

**Abstract.** The JT-60SA device has been designed as a highly shaped large superconducting tokamak with variety of plasma actuators (heating, current drive, momentum input, stability control coils, RMP coils, W-shaped divertor, fuelling, pumping etc) in order to satisfy the central research needs for ITER and DEMO. In the ITER- and DEMO-relevant plasma parameter regimes and with the DEMO-equivalent plasma shapes, JT-60SA quantifies the operation limits, plasma responses and operational margins in terms of MHD stability, plasma transport, high energy particle behaviors, pedestal structures, SOL & divertor characteristics. By integrating advanced studies in these research fields, the project proceeds ‘simultaneous & steady-state sustainment of the key performances required for DEMO’ with integrated control scenario development.

## 1. Introduction

Construction of JT-60SA [1-3] has been conducted as a joint program between the Broader Approach Satellite Tokamak program implemented by Europe and Japan, and the Japanese national program. The project mission of JT-60SA is to contribute to early realization of fusion energy by supporting exploitation of ITER [4] and by complementing ITER with resolving key physics and engineering issues for DEMO reactors [5]. Towards economically attractive steady-state DEMO reactors, the nuclear fusion research should establish reliable control schemes of burning high  $\beta$  high bootstrap current fraction plasmas. From the view point of burning plasma development, which is the main mission of ITER, satellite devices are required to support ITER by flexible exploration in the ITER-relevant plasma parameter (such as the non-dimensional parameters) regime. From the view point of high  $\beta$  high bootstrap current fraction ( $f_{BS}$ ) plasmas, an integrated research program at high values of  $\beta_N$  and  $f_{BS}$  exceeding ITER is required. In order to satisfy these requirements, the JT-60SA device and its research project have been designed.

This paper summarizes capabilities of JT-60SA for these studies based on assessment of research needs for ITER and DEMO [6]. In this paper, we refer to the Slim-CS design [5] as a typical example of DEMO reactor.

## 2. Plasma Regimes of JT-60SA

The JT-60SA device is capable of confining break-even-equivalent class high-temperature deuterium plasmas lasting for a duration (typically 100 s) longer than the timescales characterizing the key plasma processes, such as current diffusion and particle recycling, with superconducting toroidal and poloidal field coils. JT-60SA also pursues full non-inductive steady-state operations with high values of  $\beta_N$  exceeding the no-wall ideal MHD stability limits (Fig.1, Fig.2(a)). In order to satisfy these requirements, the JT-60SA device has been designed to realize a wide range of plasma equilibria, with the capability to produce both single and double null configurations, covering a DEMO- equivalent high plasma shaping

factor of  $S (= q_{95}I_p/(aB_t)) \sim 7$  and a low aspect ratio of  $A \sim 2.5$  at the maximum plasma current of  $I_p=5.5$  MA and additional heating power up to 41 MW.

The typical parameters of JT-60SA are shown in Table 1. The maximum plasma currents are 5.5 MA with highly shaped configurations (in case of the double null (DN) case,  $A=2.5$ ,  $\kappa_x=1.95$ ,  $\delta_x=0.53$ ) and 4.6 MA for an ITER-shaped configuration ( $\kappa_x=1.81$ ,  $\delta_x=0.43$ ). Inductive operations at  $I_p=5.5$  MA for the flat top duration of 100 s are possible with the available flux of  $\sim 9$  Wb. The heating system provides 34 MW of NB injection and 7 MW of ECRF. With these capabilities, JT-60SA enables explorations in ITER- and DEMO-relevant plasma regimes in terms of the non-dimensional parameters (such as the normalized poloidal gyro radius  $\rho^*$ , the normalized collisionality  $\nu^*$  (Fig.2(b)) together with high densities in the range of  $1 \times 10^{20}/m^3$ .

In DEMO reactors, we have to sustain high values of the energy confinement improvement factor (the HH-factor), the normalized beta  $\beta_N$ , the bootstrap current fraction  $f_{BS}$ , the

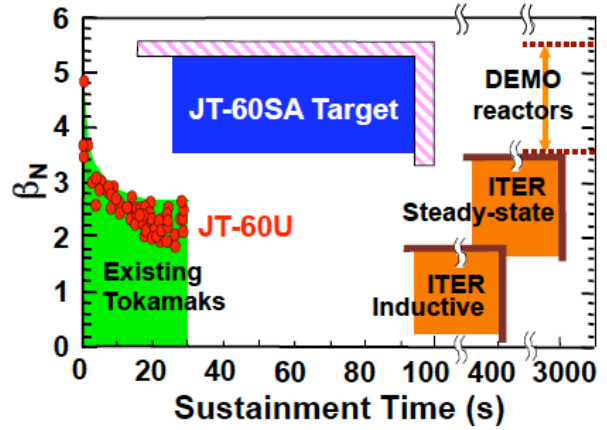


Fig.1 High  $\beta_N$  target regime of JT-60SA

Table 1. Typical plasma parameters of JT-60SA

Plasma Parameter	Full $I_p$ 5.5MA			ITER-Shape 34MW	High- $\beta_N$ full-CD	
	DN 41MW	SN 41MW	SN high-ne		Case 1	Case 2
Major Radius R (m)	2.96	2.96	2.96	2.93	2.96	2.96
Minor Radius a (m)	1.18	1.18	1.18	1.14	1.12	1.12
Plasma Current $I_p$ (MA)	5.5	5.5	5.5	4.6	2.3	2.1
Toroidal Field $B_0$ (T)	2.25	2.25	2.25	2.28	1.72	1.62
Plasma Aspect Ratio A	2.5	2.5	2.5	2.6	2.6	2.6
Plasma Elongation $\kappa_x, \kappa_{95}$	1.95, 1.77	1.87, 1.72	1.86, 1.73	1.81, 1.70	1.90, 1.83	1.91, 1.84
Plasma Triangularity $\delta_x, \delta_{95}$	0.53, 0.42	0.50, 0.40	0.50, 0.40	0.41, 0.33	0.47, 0.42	0.45, 0.41
Shape Factor S	6.7	6.3	6.2	5.7	7.0	7.0
Safety Factor $q_{95}$	3.2	3.0	3.0	3.2	5.8	6.0
Plasma Volume ( $m^3$ )	132	131	131	122	124	124
Total Heating Power (MW)	41	41	30	34	37	31
N-NB(MW)	10	10	10	10	10	6
P-NB(MW)	24	24	20	24	20	17
ECH(MW)	7	7	-	-	7	7
Assumed HH-factor	1.3	1.3	1.1	1.1	1.3	1.38
Stored Energy(MJ) th, fast	22.4, 4.0	22.2, 4.0	21.1, 1.3	18.0, 1.5	8.4, 2.7	8.1, 1.7
$\langle Te \rangle, Te(0)$ (keV)	6.3, 13.5	6.3, 13.5	3.7, 7.9	3.7, 8.0	3.3, 6.7	2.9, 5.8
$\langle Ti \rangle, Ti(0)$ (keV)	6.3, 13.5	6.3, 13.5	3.7, 7.9	3.7, 8.0	3.4, 7.1	3.1, 6.1
ne-bar, ne(0) ( $10^{20}/m^3$ )	0.56, 0.77	0.56, 0.77	0.9, 1.23	0.81, 1.11	0.50, 0.66	0.53, 0.79
Normalized Density $n_e/n_{GW}$	0.5	0.5	0.8	0.8	0.85	1.0
$\tau_E$ (s) thermal, total	0.54, 0.64	0.54, 0.64	0.68, 0.75	0.52, 0.57	0.23, 0.31	0.25, 0.30
Normalized Beta $\beta_N$	3.1	3.1	2.6	2.8	4.3	4.3
Toroidal Beta $\beta_t$ (%)	6.5	6.5	5.4	5.0	5.1	5.0
Poloidal Beta $\beta_p$	0.85	0.81	0.67	0.82	2.0	2.1
Bootstrap current fraction	0.29	0.28	0.25	0.30	0.68	0.79
Non inductive CD fraction	0.51	0.5	0.36	0.43	1	1
Normalized Gyroradius $\rho_p^*$	0.020	0.019	0.015	0.018	0.036	0.037
Normalized Collisionality $\nu^*$	0.014	0.014	0.063	0.059	0.043	0.059
Flat top duration (s)	100	100	100	100	100	100

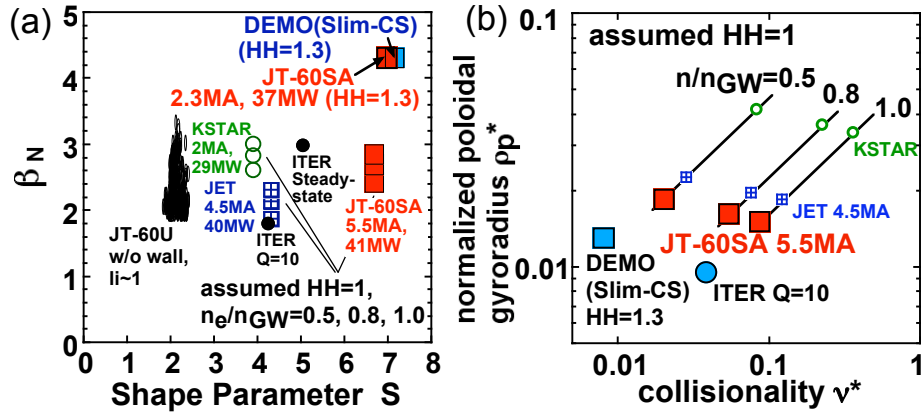


Fig.2 Non dimensional parameter regimes of JT-60SA: (a)  $\beta_N$  and shape parameter  $S$ , (b) normalized poloidal gyroradius and normalized collisionality.

non-inductively driven current fraction, the plasma density normalized to the Greenwald density, the fuel purity, and the radiation power normalized to the heating power simultaneously in the steady-state [7]. However, such a high ‘integrated performance’ has never been achieved so far. The most important goal of JT-60SA for DEMO is to demonstrate and sustain this integrated performance. JT-60SA allows exploitations of full non-inductive steady-state operations with 10MW/ 500keV tangential N-NBCD and 7 MW of ECCD. Table 1 shows two examples. Assuming HH=1.3 (case 1), the expected  $I_p$  for a high  $\beta_N=4.3$  full non-inductive current drive operation is 2.3MA ( $f_{BS} = 0.66$ ) with  $P_{heat} = 37$  MW (N-NB 10 MW, PNB 20 MW, and EC 7 MW). Assuming HH=1.38 (case 2), a full non-inductive operation with  $f_{BS} = 0.79$  and  $\beta_N = 4.3$  is expected at  $I_p=2.1$ MA and  $f_{GW} (=n_e/n_{GW})=1$  with a medium NNB current drive power of 6MW. In this case, controllability of high  $\beta_N$  high  $f_{BS}$  plasmas can be studied by utilizing the remaining margin of the NNB power. These plasma regimes satisfy the research goal of the highly integrated performance as shown in Fig.3.

### 3. Capabilities of plasma actuators

JT-60SA has strong heating and current drive power allowing variety of heating, current-drive, and momentum- input combinations. The total heating power is 41 MW, which consists of 34 MW of NB injection (24 MW of P-NB and 10 MW of N-NB, see Fig.4) and 7 MW of ECRF. The positive ion source based neutral beams (P-NBs) at 85 keV consist of 2 units of co-tangential beams (4 MW), 2 units of counter-tangential beams (4 MW), and 8 units of near perpendicular beams (16 MW). The negative ion source based neutral beam (N-NB) system provides 10 MW/500 keV co-tangential injection. The N-NB injection trajectory is off-axis for optimization of the weak / negative magnetic shear plasmas. The 7 MW/110 GHz ECRF system allows a real time

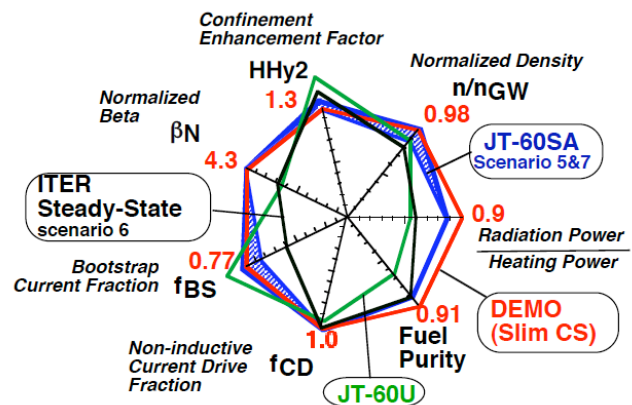


Fig.3. Integrated plasma performance of JT-60SA(blue) compared with DEMO Slim-CS (red), ITER steady-state (black) and a JT-60U simultaneous achievement[8]. In all cases,  $q_{95}=5.5 - 6$ .

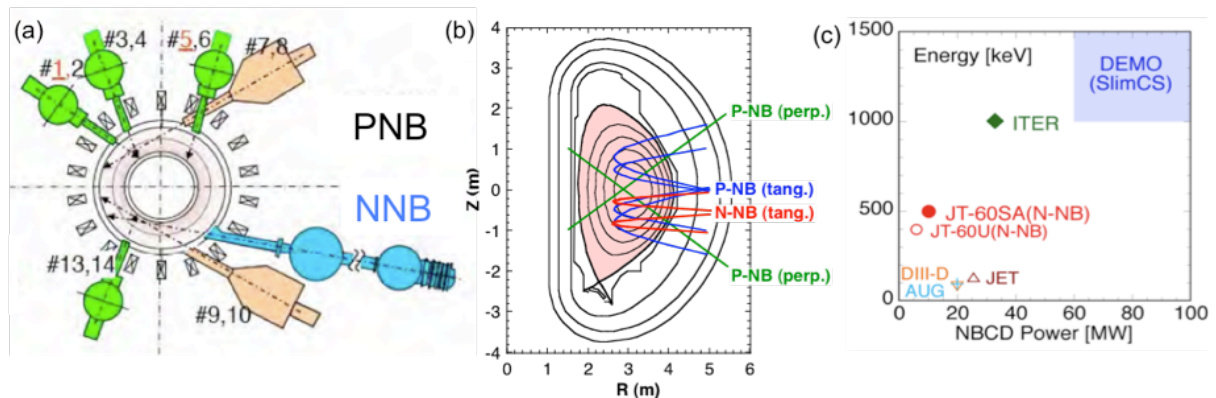


Fig. 4. (a) The JT-60SA NBI system, (b) NB injection trajectories for PNBs and NNBs, and (c) accelerating voltage and power of NB injection for tokamaks

control of the deposition location by steerable mirrors with high frequency modulation capability ( $>5$  kHz).

JT-60SA studies power and particle handling at the full injection power of 41 MW for 100 s using the lower and upper water-cooled divertors compatible with the maximum heat flux of  $15 \text{ MW/m}^2$  [9]. The W-shaped divertor with a V-corner enhances divertor radiation. The divertor pumping speed can be changed by 8 steps up to  $100 \text{ m}^3/\text{s}$  for the lower divertor. The fuelling system consists of the main and divertor gas puffing for multiple gas species and high- and low-field-side pellet injection.

In order to allow exploitations of high beta regimes, JT-60SA is equipped with the stabilizing shell matched to the high shape factor configurations, the resistive wall mode (RWM) stabilizing coils, and the error field correction/generation coils [10] in addition to the high power heating & current drive & momentum-input systems. The error field correction/generation coils also allow the resonant magnetic perturbation (RMP) for type-I ELM suppression for the various plasma regimes.

At present, 26 systems are in preparation for plasma diagnostics with high space and time resolutions sufficient for conducting the physics research and plasma real-time controls. In particular, by combining these diagnostics systems with the plasma actuators listed above, advanced real-time control schemes for the highly self-regulating plasmas will be developed.

## 4. JT-60SA Research Regimes for ITER and DEMO

### 4.1 Non-inductive Current Drive

As shown in Fig.3, one of the most important goals of JT-60SA is achievement of the steady-state high integrated performance with full non-inductive current drive at high  $f_{BS}$ . Figures 5 (a) and (b) show the full non-inductive current drive capability of JT-60SA using 10MW of N-NBCD, 7MW of ECCD and 20MW of P-NB heating [11]. The sustainable  $I_p$  is 2 – 3MA in the range of  $HH=1.1 - 1.6$  and  $f_{GW} (=n_e/n_{GW})=0.5 - 0.9$ . At  $HH=1.3$  and  $f_{GW}=0.85$ , the full non-inductive current drive is achievable at  $I_p=2.3\text{MA}$  ( $B_t=1.7\text{T}$ ) with  $f_{BS}=0.66$  and  $\beta_N=4.3$  (the high  $\beta_N$  case 1 in Table 1). Figures 5 (c) and (d) show the radial profiles of  $T_e$ ,  $T_i$ ,  $n_e$ , the driven currents and the safety factor for this reversed shear plasma, where the core profile shapes of  $T_e$ ,  $T_i$  and  $n_e$  are based upon JT-60U experiment and the pedestal width is given by the EPED1 model [12]. The assumed pedestal is stable for the peeling-ballooning mode at  $n < 40$  (MARG2D [13]). With an ideal wall, this plasma having  $\beta_N=4.3$  ( $>$  no-wall limit  $\sim 2$ ) is stable against  $n \leq 4$  kink ballooning modes (MARG2D). When we use the CDBM model [14] for transport evaluation in a similar plasma, the predicted HH is 1.5.

However, in order to establish a control scenario towards DEMO, we have to keep a margin for the current drive power. When we assume  $HH=1.38$  (still lower than the CDBM prediction), a full non-inductive operation with  $f_{BS}=0.79$  and  $\beta_N=4.3$  is expected at  $I_p=2.1MA$  and  $f_{GW}=1$  with 6MW of N-NBCD, 7MW of ECCD and 17MW of P-NB heating (the high  $\beta_N$  case 2 in Table 1). In this case, controllability of the high  $\beta_N$  high  $f_{BS}$  plasma can be studied by utilizing the remaining margin of 4MW N-NB. In addition, an attractive burning plasma simulation can be carried out. When we inject the P-NB ( $\sim 17MW$ ) and ECH ( $\sim 7MW$ ) power in proportion to the DD neutron production (or to  $n_i^2 T_i^2$ ) by a real time feedback, we can simulate a  $Q\sim 20$  ( $=24 \times 5/6$ ; simulated  $\alpha$ -power of 24MW and external N-NBCD power of 6MW) burn control in this high  $\beta_N$  high  $f_{BS}$  regime.

Another important research issue is non-inductive plasma current rise for minimization of the CS coil for DEMO. JT-60SA explores this subject by ‘high  $f_{BS}$  + N-NB CD’.

### 4.2 Integrated Plasma Control

The fusion plasma is a self-regulating combined system. The most important objective of JT-60SA is to understand this system and to establish suitable control schemes, and to demonstrate steady-state sustainment of the integrated performance shown in Fig.3. The key points are as follows:

- i) Fusion plasmas are governed by strong linkages among radial profiles of the plasma current density, the plasma pressure and the plasma rotation in the core and in the pedestal. This self-regulation becomes stronger at higher  $\beta$ .
- ii) Fusion plasmas have a global or semi-global nature (such as structure formation, stiff radial profiles etc.) combining the whole plasma regions from the core to the pedestal.
- iii) The pedestal plasma, giving the boundary condition to the core, and SOL / divertor plasmas have also a strong linkage including plasma processes, neutral particle processes, and plasma-material interactions.

We have to control this system with small fractions of external drives. Figure 6 shows  $\beta_N$  and  $f_{BS}$ , and  $\beta_N$  and  $f_{BS}/(1-f_{BS}) =$  the ratio of the self-driven current to the external driven current. When  $f_{BS}$  is 80% ( $\sim$ DEMO), the ratio ‘self

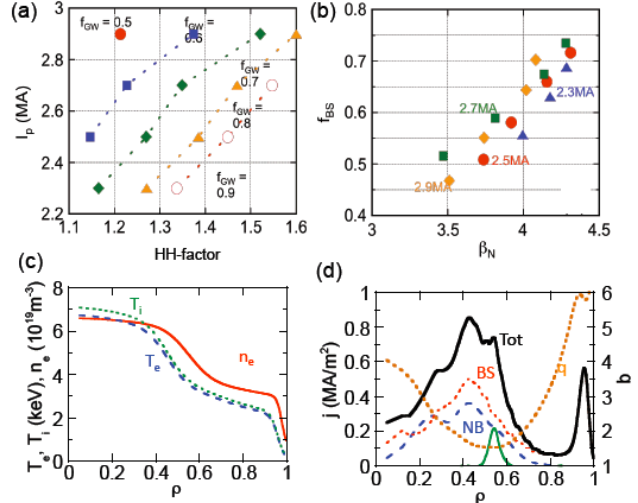


Fig.5. JT-60SA full non-inductive CD regimes: (a) Driven  $I_p$  against  $HH$  with various  $f_{GW} = n_e/n_{GW}$ , (b) corresponding  $f_{BS}$  vs  $\beta_N$ . (c) and (d) show the profiles of  $T_e$ ,  $n_e$ ,  $T_i$  and driven current for the  $I_p=2.3MA$ ,  $HH=1.3$  case (high  $\beta_N$  case 1 in table 1).

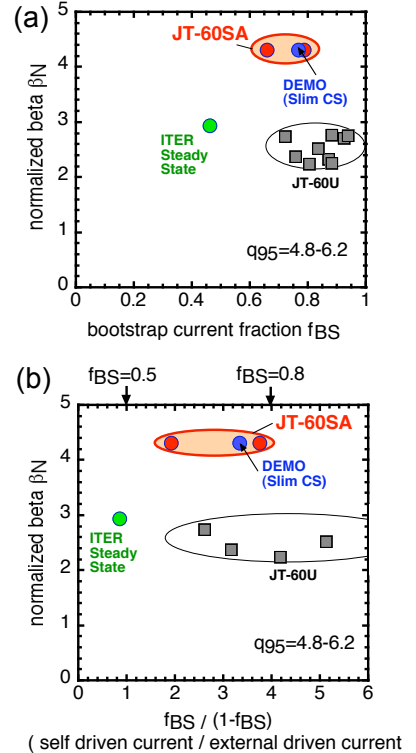


Fig.6. (a)  $\beta_N$  and the bootstrap current fraction  $f_{BS}$ . (b)  $\beta_N$  and  $f_{BS}/(1-f_{BS}) =$  self driven current / external driven current for JT-60SA, ITER steady-state, and JT-60U achievements.

driven : external driven' = 4 : 1. With this small fraction of the external drive, the 'self regulating combined system' should be controlled in DEMO. As shown in Fig.6, JT-60SA can explore such controllability.

Another important operation regime is so-called 'hybrid operation'. With a full bore single null configuration at  $I_p=4.4$  MA,  $q_{95}\sim 4.2$ ,  $f_{GW}\sim 0.7$ ,  $HH\sim 1.1$  with 34 MW injection, a  $q$  profile with  $q > 1$  except very vicinity of the plasma center can be obtained in JT-60SA [11].

By utilizing the capabilities mentioned above, JT-60SA promotes the following studies for establishment of the integrated control schemes: JT-60SA identifies operational boundaries, decides control margin, clarifies plasma responses, selects the optimum and minimum set of actuators and diagnostics applicable to DEMO, determines the control logic (such as non-linear gain matrix and real time prediction etc.) and demonstrates the real-time control in long pulse discharges for ITER and DEMO.

Controllability of plasma equilibrium including recovery after plasma events has to be clarified within engineering limitations of the super conducting coil system. Particle controls have to be demonstrated under saturated wall conditions. Current profile controls have to be demonstrated around the relaxed current profile with bootstrap current fraction  $< 50\%$  (for ITER) and  $> 50\%$  (for DEMO).

These experiments should be conducted in the ITER and DEMO-relevant regimes in terms of plasma shape, non-dimensional parameters together with high densities in the range of  $1 \times 10^{20}/m^3$ . This is because the key processes in the pedestal, SOL, and divertor plasmas involve atomic processes determined by dimensional parameters such as  $T_e$  and  $n_e$ .

### 4.3 MHD Stability and Control Studies

High  $\beta$  plasmas are stabilized with the stabilizing shell, the RWM stabilizing coils, and the error field correction coils in addition to the heating & current drive & momentum- input controls. For DEMO, JT-60SA demonstrates long pulse high  $\beta_N > 4$  plasmas and determines the stability boundary for DEMO-equivalent highly shaped plasmas (Fig.2(a)). At the same time, JT-60SA clarifies the minimum requirements for RWM stabilization by plasma rotation without using control coils, and quantifies the operational margin. For ITER, JT-60SA optimizes effective real-time stabilization schemes for  $m/n=2/1$  and  $3/2$  NTMs by ECCD using movable mirrors and high frequency modulation at  $> 5$  kHz for the high  $I_p$  and low  $q_{95}$  plasmas having the ITER-relevant non-dimensional parameters. JT-60SA explores disruption mitigation by applying magnetic fluctuations or massive gas injection in high  $I_p$  large bore plasmas for ITER and DEMO.

### 4.4 Confinement and Transport Studies

The confinement and transport (heat, particle, momentum) characteristics including detailed physics processes such as plasma turbulence are clarified for understanding of the self-regulating combined system and for establishment of the integrated plasma control at the ITER- and DEMO- relevant non-dimensional parameters such as low values of  $\rho^*$  and  $\nu^*$  as shown in Fig.2(b). In addition, these studies have to be conducted with ITER and DEMO relevant heating conditions; such as dominant electron heating and low central fueling enabled by N-NB and ECH, and low external torque input enabled by N-NB, ECH, perpendicular P-NBs and balanced injection of CO and CTR tangential P-NBs. Effects of the electron heating fraction (see Fig.7) and plasma rotation are also clarified by changing combinations of these heating systems. Particle confinement and exhaust, in particular high  $Z$

impurities, in high confinement (HH=1.3 – 1.4) plasmas should be clarified. JT-60SA promotes burning simulation by using variety of NBs, and clarifies plasma responses and controllability by applying the plasma controls planned in ITER. The key point is whether the fueling control can be a reliable burn control scheme.

**4.5 High Energy Particle Studies**

Utilizing the high power and high energy N-NB, JT-60SA can clarify stability of Alfvén Eigenmodes (AEs) and effects of AEs on fast ion transport at ITER and DEMO-equivalent values of the fast ion  $\beta=0.2 - 1\%$  with fast ion velocity / Alfvén velocity = 1.5 - 2 (Fig.8) over a wide range of the safety factor profile from monotonic to reversed. Interactions between high energy ions and MHD instabilities, such as sawteeth, NTMs, EWMs (Energetic particle driven Wall Mode), RWMs, are studied using N-NB. Current drive capability is studied using the 500 keV 10 MW N-NB (Fig.4(c)). Off axis current drive and profile controllability are evaluated with off-axis N-NB (Fig.4(b)).

**4.6 Pedestal studies**

For ITER, the L-H transition conditions, such as the threshold power, can be quantified for H, He and D plasmas in the high  $I_p$  (4-5.5MA) and high density ( $n_e \leq 1 \times 10^{20}/m^3$ ) regime in particular with the ITER-like plasma shape and high power electron heating by ECH and NNB. The pedestal structure, the width and the height, and inter-ELM transport are clarified over wide ranges of  $I_p$  and density in order to predict the performance of Q=10 plasmas. Type-I ELM energy loss is a function of the pedestal collisionality  $\nu^*$ . Since JT-60SA pedestal plasmas can cover a wide range of  $\nu^*$  as shown in Fig.9, JT-60SA clarifies the type-I ELM energy loss and the transient heat load on to the divertor plates. At the same time, effects of RMP and pellet pace making for ELM mitigation are clarified in such ITER-relevant conditions.

In order to predict the pedestal characteristics for DEMO, the pedestal structure, the ELM stability and the inter-ELM transport are clarified over wide ranges of plasma shape up to DEMO-equivalent shape. The high triangularity shape of JT-60SA plasmas for the high  $f_{BS}$  operation locates well inside the region suitable for appearance of small ELMs (Grassy ELMs) as

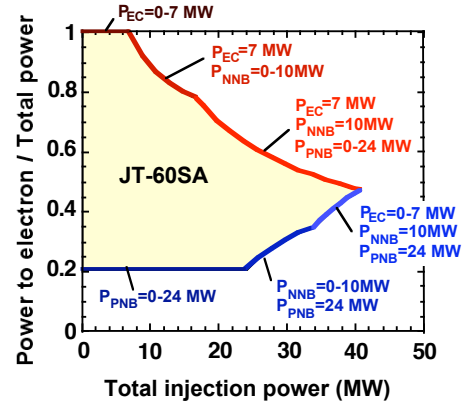


Fig.7. Fraction of the electron heating power to the total heating power

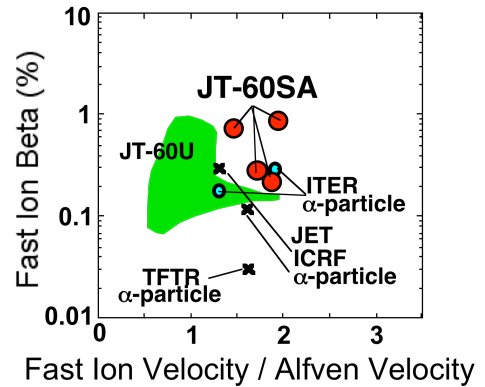


Fig.8. Fast ion beta vs. fast ion velocity normalized to Alfvén velocity

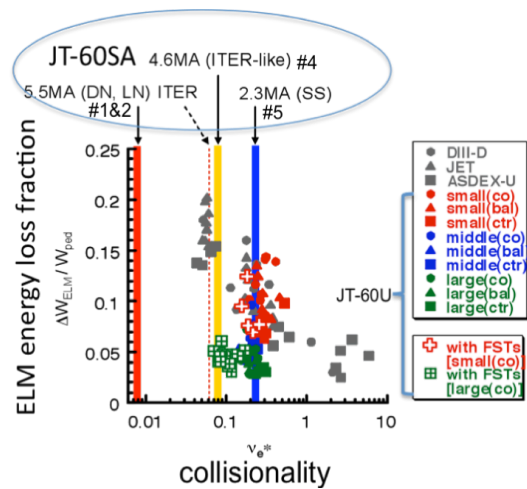


Fig.9. ELM energy loss fraction to the pedestal stored energy vs. the pedestal collisionality

shown in Fig.10. JT-60SA expands the Grassy ELM regime and demonstrates ELM mitigation without RMP.

#### 4.7 SOL, Divertor and Plasma-Material Interaction

One of the most important mission of JT-60SA is to demonstrate divertor power and particle handling with simultaneous sustainment of the high core plasma performances under a high heating power (<41MW) for a long time duration (<100s). The JT-60SA device is designed to produce equilibria aligned for the ITER-like divertor structure ('2cm SOL' enters the vertical divertor target for all cases shown in Table 1). The W-shaped divertor with a V-corner enhances divertor radiation. The peak heat flux is predicted to be suppressed within the monoblock capability (15 MW/m<sup>2</sup>) by gas puffing for 41 MW injection [16]. JT-60SA demonstrates fuel and impurity particle controls by utilizing variety of the fuelling and pumping systems. Compatibility of the radiative divertor with impurity seeding and sufficiently high fuel purity in the core plasma should be demonstrated. The key point is to clarify whether a wide range of the divertor plasma controllability can be realized independently of the main plasma condition by utilizing the pumping and particle seeding from the divertor area as shown in Fig.11. Metallic divertor targets and first wall together with an advanced shape divertor will be installed in the extended research phase in order to demonstrate the high integrated performance with metallic wall.

#### References

- [1] S. Ishida et al., Fusion Engineering and Design.
- [2] S. Ishida et al., this conference, OV/P-4.
- [3] P. Barabaschi et al, this conference, FTP/2-1
- [4] 'Progress in the ITER Physics Basis', Nucl. Fusion 47 (2007) S1.
- [5] K. Tobita et al., Nucl. Fusion 49 (2009) 075029.
- [6] Y. Kamada et al., J. Plasma Fusion Res. SERIES, Vol. 9, (2010) 641.
- [7] Y. Kamada and JT-60 Team, Nucl. Fusion 41 (2001) 1311.
- [8] Y. Sakamoto et al., Nucl. Fusion 49 (2009) 095017.
- [9] S. Sakurai et al., this conference, FTP/P1-29
- [10] M. Takechi et al., this conference, FTP/P6-30
- [11] S. Ide et al., Proc. of the 37th European Physics Society Conf. on Plasma Physics, 2010, O3.108.
- [12] P.B. Snyder et al., Nucl. Fusion 49 (2009) 085035.
- [13] N. Aiba et al., Comput. Phys. Commun. 175 (2006) 269.
- [14] A. Fukuyama, et. al., Plasma Phys. Control. Fusion 37 (1995) 611.
- [15] N. Oyama et al., Plasma Phys. Control. Fusion 49 (2007) 273.
- [16] H. Kawashima et al., 19<sup>th</sup> PSI (2010) P3-24, to be published in J. Nucl. Mater.

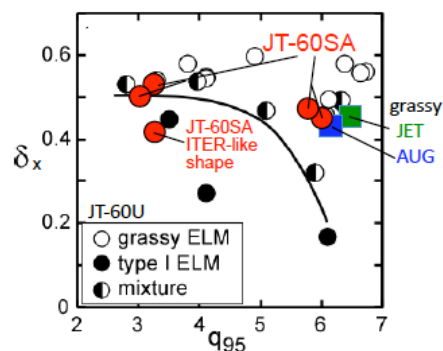


Fig.10. The Grassy ELM regime in JT-60U[15], AUG, JET and the JT-60SA operation regime

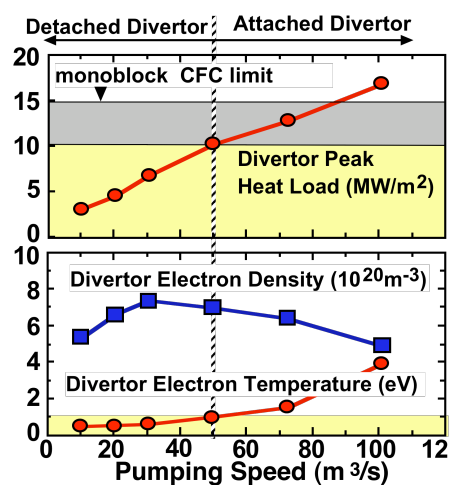


Fig.11 Effect of divertor pumping speed ( $S$ -pump): By changing  $S$ -pump, the divertor heat load can be controlled with constant separatrix-mid-plane density.